Showcasing research from Professor Craig Townsend's laboratory, Department of Chemistry, The Johns Hopkins University, Baltimore, MD, USA. Image designed and illustrated by Anneliese Faustino.

Stereochemical course of cobalamin-dependent radical SAM methylation by TokK and ThnK

The stereochemical course of only a handful of cobalamin-dependent radical S-adenosylmethionine methylases has been determined, with both inversion and retention of configuration having been observed. The X-ray structure of TokK, a canonical member of this family involved in carbapenem antibiotic biosynthesis, is ambiguous as to the stereochemical identity of the abstracted substrate hydrogen. Here we present the synthesis of deuterated carbapenam probes of high isotopic and diastereomeric purity and determine that methyl transfer proceeds cleanly by inversion of absolute configuration at C6.
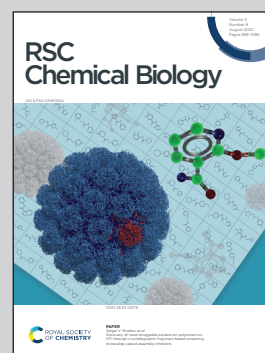
ROYAL SOCIETY OF CHEMISTRY

PAPER

Check for updates

Stereochemical course of cobalamin-dependent radical SAM methylation by TokK and ThnK†

Michael S. Lichstrahl, [ID] ‡ Craig A. Townsend [ID] * and Erica K. Sinner [ID] *‡

Complex carbapenems are important clinical antibiotics for difficult-to-treat infections. An essential step in the biosyntheses of these natural products is stereospecific methylation at C6 and subsequent alkylations by cobalamin-dependent radical SAM methylases such as TokK and ThnK. We have prepared isotopically labeled substrates in a stereospecific manner and found that both homologous enzymes selectively abstract the 6-pro-*S* hydrogen, followed by methyl transfer to the opposite face to give the (6*R*)-methyl carbapenam product proceeding, therefore, by inversion of absolute configuration at C6. These data clarify an unexpected ambiguity in the recently solved substrate-bound crystal structure of TokK and have led to a stereochemically complete mechanistic proposal for both TokK and ThnK.

Introduction

TokK and ThnK are cobalamin (Cbl)-dependent radical *S*-adenosylmethionine (rSAM) methylases that catalyze sequential methylations in complex carbapenem antibiotic biosynthesis. These enzymes share 79% sequence identity and a common substrate, (2*R*,3*R*,5*R*)-pantetheinylated carbapenam (PCPM, **1**). However, TokK and ThnK differ in the number of methylations they catalyze in the biosyntheses of asparenomycin (**6**) and thienamycin (**5**), respectively (Scheme 1).[1–4] The differences in the kinetic behavior of these two enzymes have been previously discussed,[1] and the recent structural characterization of TokK greatly improved our mechanistic understanding of Cbl-dependent rSAM methyl transfer.[5] Despite these advances, however, the stereochemical course of methylation by TokK could not be determined directly from the structure.

TokK uses a [4Fe–4S] cluster to reductively cleave SAM, generating a 5′-deoxyadenosyl radical (5′-dA•), which abstracts a hydrogen atom from C6 of PCPM (**1**) to form 5′-deoxyadenosine (5′-dAH). The substrate radical is methylated by the homolytic cleavage of methylcobalamin (MeCbl), which is formed by the nucleophilic attack of cob(I)alamin on a second equivalent of SAM.[6–8] A similar mechanistic strategy is employed by the related sequential methylase CysS, which, unlike TokK and ThnK, acts on a carrier protein-bound substrate.[9] The first methylation by both TokK and ThnK yields Me-PCPM (**2**) with the *R* configuration at C6[1,2] (Scheme 1). Early

studies with the thienamycin producer showed that the methyl groups are methionine-derived.[3] This result has been confirmed by using isotopically labeled SAM in assays with ThnK, which leads to a corresponding mass shift in the methylated product.[2] Additionally, experiments with chiral-methyl methionine gave overall retention of absolute configuration in the transferred methyl group.[10] Because this result was inconsistent with direct transfer from SAM, Floss and colleagues correctly predicted the involvement of a MeCbl intermediate.

These insights notwithstanding, the identity of the hydrogen atom abstracted by the 5′-dA• generated by ThnK and TokK is unknown. Detailed *in vitro* stereochemical analysis has only been done with a small number of Cbl-dependent rSAM methylases, and has not always been straightforward. Fom3, which methylates a fosfomycin precursor, was first thought to be a nonstereoselective catalyst,[11] but upon further inspection was found to proceed with inversion of configuration.[12–14] Conversely, GenK, which is a methylase in gentamycin biosynthesis, proceeds with retention of configuration.[15] The stereochemical relationship between H-atom abstraction and methylation is likely determined by the relative placement of the substrate to 5′-dA• and MeCbl in the active site. Therefore, it was thought that structural characterization of Cbl-dependent rSAM enzymes would reveal the stereochemistry of each step of the reaction. However, due to the practical limitations of working with these enzymes, progress in this area has been slow.[16] There are currently four structurally characterized Cbl-dependent rSAM enzymes: OxsB,[17] TsrM,[18] Mmp10,[19] and TokK.[5] The first two structures solved in this small set of enzymes are mechanistic outliers, limiting their utility in connecting active site architecture and catalytic function. OxsB is thought to perform a radical ring contraction,[17,20] and TsrM is a methylase that uses an unconventional non-radical

Department of Chemistry, The Johns Hopkins University, 3400 N Charles St, Baltimore, Maryland, USA. E-mail: ctownsend@jhu.edu

‡ These authors contributed equally to this work.
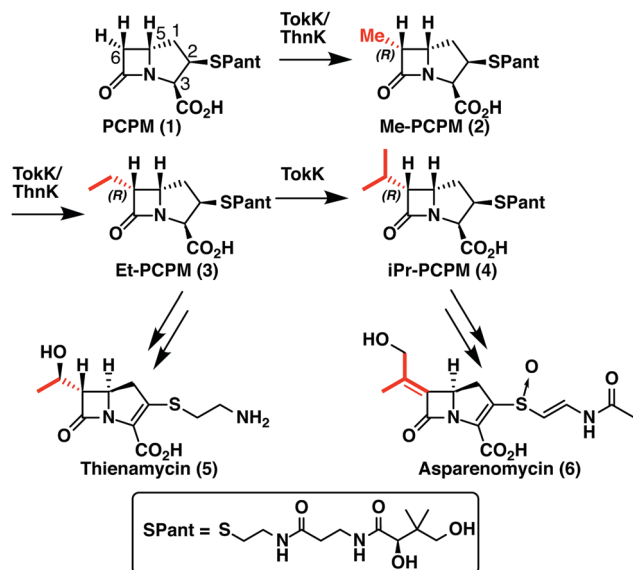
Scheme 1 Reactions catalyzed by ThnK and TokK in the biosyntheses of Thienamycin and Asparenomycin.

mechanism.[18,21,22] Moreover, OxsB was not co-crystallized with its substrate,[17] and the position of the substrate bound to TsrM is incompetent for catalysis.[18] Mmp10 was crystallized with its substrate,[19] but has a non-canonical domain architecture and does not cluster with the Cbl-dependent subfamily in a sequence similarity network of rSAM enzymes.[23] Therefore, the recently solved 1.9 Å X-ray structure of TokK co-crystallized with substrate, hydroxycobalamin, methionine, and 5′-deoxyadenosine (5′-dAH)[5] is an advance likely to be the most representative structure of the Cbl-dependent rSAM subfamily. The TokK structure clearly shows the Cbl cofactor oriented to methylate from the bottom face of the β-lactam ring to give the (6R)-Me-PCPM (**2**) product.[5] However, to our surprise, the structure did not clearly reveal which C6 hydrogen is abstracted by 5′-dA•. As shown in Fig. 1, 5′-dAH is situated approximately halfway between the two modeled C6 hydrogen atoms. It was therefore unclear if hydrogen atom abstraction

Fig. 1 Substrate–bound TokK active site with pro-*S* and pro-*R* hydrogens modeled. (PDB ID: 7KDY).

would be stereorandom or stereoselective, and if selective, which hydrogen would be preferentially removed by TokK. We set out to address this question by using the unambiguous chemical approach of examining the fate of stereospecifically deuterated substrates. Together with the structural insight into TokK, we now have a more complete picture of the mechanism of methylation by the Cbl-dependent rSAM subfamily.

Results and discussion

Synthesis of deuterated probes

To achieve highly stereoselective labeling at C6 of the carbapenam PCPM (**1**) we elected to set this stereocenter prior to formation of the β-lactam ring. The instability of the carbapenam nucleus and the functionally indistinguishable reactivity of the two C6 hydrogens precludes late-stage labeling. We therefore assessed our previous syntheses of carbapenams[1,24] to ensure both scalability and high deuterium incorporation at an earlier step. Monocyclic β-lactams **14a**/**14b** were identified as key intermediates known to be accessible from dibenzyl D-aspartate.[25] We envisioned, therefore, the preparation of diastereomeric [3-²H] D-aspartates **11a** and **11b**.

Isotopic labelling of amino acids is well precedented and many deuterated amino acid derivatives are commercially available. While the asymmetric deuteration of numerous natural and non-canonical amino acids at the α-carbon (C2) has been described,[26–28] stereoselective generation of β-carbon (C3) labeled substrates is far less common. A chemoenzymatic synthesis of both diastereomers of [3-²H] L-aspartic acid on large scale and with high incorporation of deuterium has been reported.[29] Unfortunately, the reliance on biocatalysts precludes the ability to generate unnatural D-amino acids, necessitating a fully chemical approach.

Retrosynthetic analysis of aspartic acid led us to propose tartrate as a chiral-pool starting material. While the mono-reduction of tartrate to malate has been extensively explored in the literature,[30,31] most processes rely upon single-electron mechanisms unsuitable for stereoselective introduction of deuterium at C3. We initially explored the direct reduction (D₂) of a symmetrical aziridine dicarboxylate readily accessible from tartrate,[32] in the hope that deuterium uptake from the catalyst surface would be stereospecific along one of the symmetry-equivalent edges of the aziridine. Instructively, reduction was observed to be stereorandom, which has precedence in the literature.[33] Attempts to accomplish the same transformation using alternative reducing agents were either unsuccessful or incompatible with other functional groups. Therefore, we pursued an alternative approach using a similar symmetrical heterocycle that would serve as a chiral synthon for stereospecific deuteration.

Sharpless *et al.* have previously described the reductive opening of tartrate-derived cyclic sulfates using hydride reagents, including NaBH₄.[34,35] This reduction occurs by an S_N2 mechanism and, therefore, should occur with complete inversion at the C3 stereocenter. We repeated this reduction on
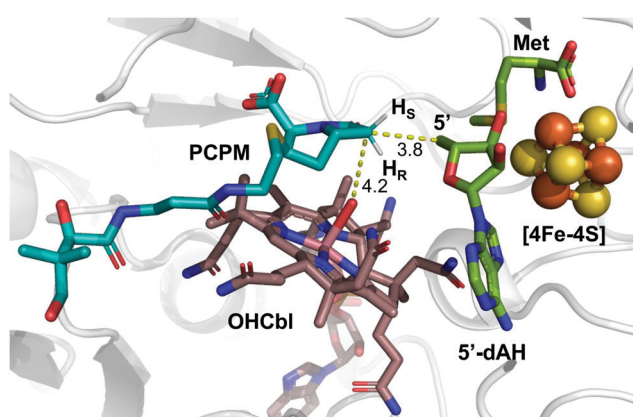
© 2022 The Author(s). Published by the Royal Society of Chemistry

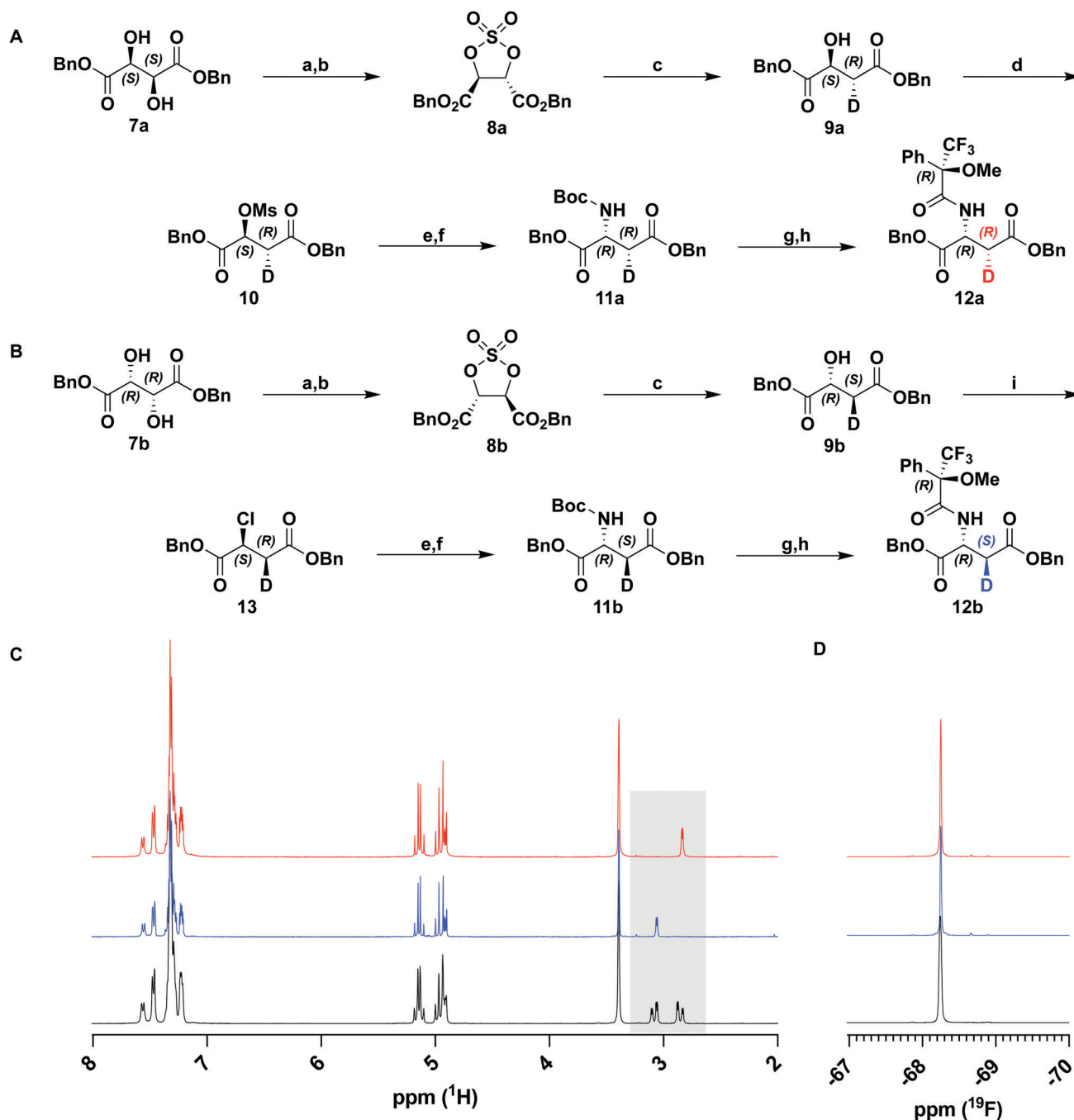*RSC Chem. Biol.*, 2022, **3**, 1028–1034 | **1029**

Fig. 2 (A) and (B) Preparation of deuterated D-aspartates and their respective Mosher amides. *Reagents and conditions*: (a) SOCl$_2$, DMF (cat.), DCM, 0 to 50 °C, 30 min; (b) NaIO$_4$, RuCl$_3$·3H$_2$O (cat.), CH$_3$CN, H$_2$O, rt, 1 h; (c) NaBD$_4$, DMAc, rt, 1 h, then, (NH$_4$)$_2$SO$_4$, H$_2$SO$_4$, Et$_2$O, rt, 24 h; (d) MsCl, DIPEA, DCM, 0 °C, 1.5 h; (e) NaN$_3$, DMSO, rt, 18 h; (f) SnCl$_2$, dioxane, H$_2$O, 0 °C to rt, 2 h, then Boc$_2$O, NaHCO$_3$, 0 °C to rt, 18 h; (g) TFA, DCM, rt, 2 h; (h) (S)-(+)-MTP–Cl, NEt$_3$, DMAP, DCM, rt, 2 h; (i) SOCl$_2$, pyridine, CHCl$_3$, 0 to 60 °C, 4 h. (C) ^{1}H NMR spectra of **12a** (red), **12b** (blue), and unlabeled control (black). (D) ^{19}F NMR spectra of **12a** (red), **12b** (blue), and unlabeled control (black).

cyclic sulfates **8a** and **8b** derived from dibenzyl D- and L-tartrate with NaBD$_4$ (Fig. 2(A) and (B)). Following hydrolysis of the intermediate alkyl sulfate and purification, ^{1}H-NMR analysis of the product malates showed a simplified coupling pattern consistent with excellent deuterium incorporation (96–99%, over several preparations, confirmed by HRMS) and the expected stereoinversion. This procedure could be used to

prepare both the (2*S*,3*R*)- and (2*R*,3*S*)-enantiomers of dibenzyl malate (**9a** and **9b**).

With deuterium installed stereospecifically and at a high level, we proceeded to prepare the desired D-aspartate, and further the β-lactam. Against expectation, we found very few examples of the conversion of malate to aspartate in the literature. Most precedence involves the inversion of triflates

1030 | *RSC Chem. Biol.*, 2022, **3**, 1028–1034

© 2022 The Author(s). Published by the Royal Society of Chemistry

with hydroxylamine[36] or hydrazine[37] derivatives. Although these transformations proceeded in high yields and optical purity, the reduction of the product derivatives would not be compatible with our ester protecting groups. Instead, we chose to use azide as a nucleophilic source of nitrogen in analogous substitution reactions. Activation of **9a** as mesylate **10** was accomplished in high yields with minimal elimination and was followed by displacement by NaN$_3$. Substitution by azide gave an inseparable *ca.* 2:1 mixture of substitution and elimination products. Rather than attempt to purify the reaction product, the crude material was subjected to a one-pot tin(II) chloride-mediated reduction and subsequent Boc protection. The protected D-aspartate **11a** was easily purified and isolated in 55% yield over two steps (Fig. 2(A)).

Having prepared the D-aspartate from D-tartrate derived **9a**, we sought to achieve the same using the L-tartrate derived **9b** (Fig. 2(B)). To achieve the desired stereochemistry at C2, it was necessary to perform a double-inversion at this center. SOCl$_2$/pyridine simultaneously accomplished the first inversion and generation of a leaving group in **13**. Appel bromination was initially explored to effect a similar inversion and generate a better leaving group, but resulted in significant racemization at C2, a known phenomenon owing to repeated bromide displacements in such activated systems.[36] Using an identical procedure as above, chloride **13** was displaced with azide and telescoped to **11b**. A reduced yield was obtained in this step due to substantially greater elimination (>60%) in the azidation reaction. This observation suggests that both leaving group identity and stereochemistry of the adjacent deuterium significantly affect the ratio of substitution and elimination products.

To verify the desired stereochemistry and optical purity at C2 in **11a** and **11b**, we converted each to its respective (*R*)-Mosher amide **12a** and **12b**. Comparison of their ^{1}H NMR spectra as shown in Fig. 2(C) demonstrated that the compounds were diastereomeric at C3. Further comparison of the corresponding ^{19}F NMR spectra (Fig. 2(D)) to the Mosher amide prepared from unlabeled dibenzyl D-aspartate confirmed the stereochemistry at C2. Following deprotection and deprotonation to the free amine, an established procedure[25] was slightly modified to efficiently cyclize both substrates to the diastereomeric [3-^{2}H]-β-lactams **14a** and **14b** (Fig. 3(A)). Direct comparison of their ^{1}H-NMR spectra, as well as the unlabeled reference compound, further secured the assigned stereochemistries (Fig. 3(B)). A simple doublet was observed at C4 of the azetidinone with *J* = 6.0 or 2.8 Hz for **14a** and **14b**, respectively, in accord with Karplus dihedral angle dependence.[38] These key intermediates were separately elaborated to the correspondingly labeled PCPM isotopologues using a strategy similar to that described previously (Scheme 2).[1,24] Briefly, after removal of the benzyl ester by hydrogenolysis to afford **15a** and **15b**, each carboxylic acid was subjected to an Arndt-Eistert homologation.[39] The resultant **16a** and **16b** were activated by carbonyldiimidazole (CDI) and extended by the decarboxylative addition of Mg(mono-PNB malonate)$_2$.[40] Subsequent removal of the silane resulted in the formation of **17a** and **17b**, which were diazotized to **18a** and **18b**. This transformation enabled rhodium(II)
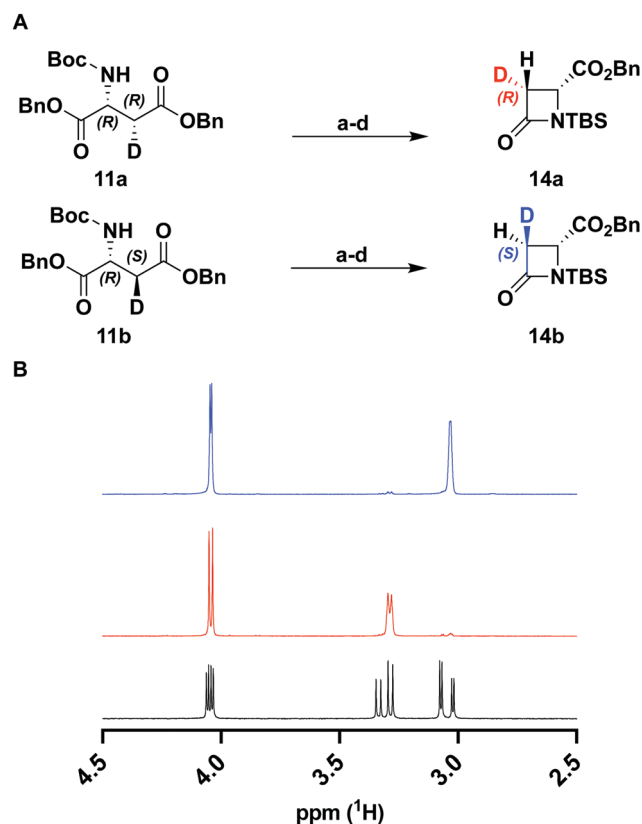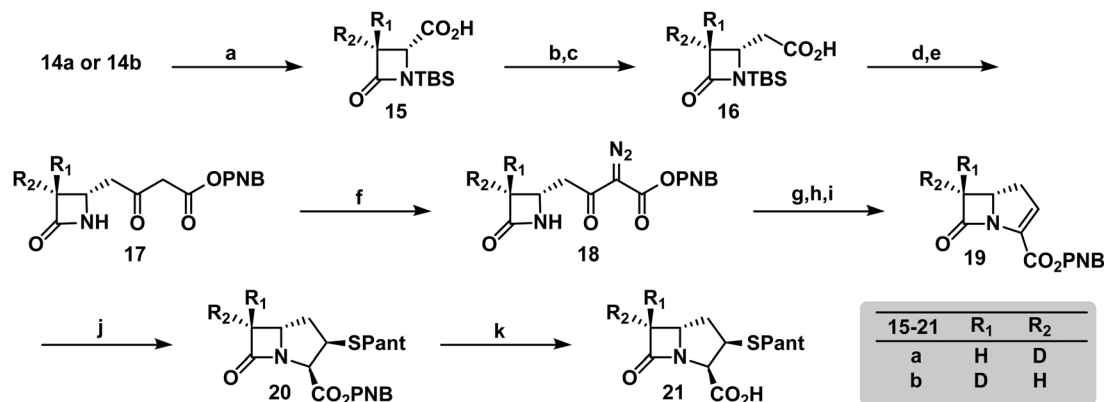

Fig. 3 (A) synthesis of β-lactams from D-aspartates. *Reagents and conditions*: (a) TFA, DCM, rt, 2 h; (b) 1 M K$_2$CO$_3$, DCM, rt, 45 min; (c) TBSOTf, NEt$_3$, DCM, rt, 4 h; (d) *t*BuMgCl, Et$_2$O, 0 °C to rt, 16 h. (B) ^{1}H NMR spectra of **14a** (red), **14b** (blue), and unlabeled control (black).

catalyzed carbene insertion to form the 5-membered ring as a 2-oxocarbapenam, which was reduced, mesylated, and eliminated in each case to give carbapenems **19a** and **19b**. Pantetheine 1,4 addition was followed by HPLC separation of the C2 diastereomers to yield **20a** and **20b**. Hydrogenolysis of the PNB esters gave PCPMs **21a** and **21b** in 21 steps from dibenzyl tartrate.

ThnK and TokK are stereoselective

TokK and ThnK were expressed and purified as reported previously.[41] Each enzyme (100 μM) was incubated with each substrate (1 mM) for 90 min and the formation of products was monitored by UPLC-HRMS. By using a substrate concentration 10-fold higher than the enzyme concentration, the first methylation in the sequence is the dominant reaction for each enzyme, giving Me-PCPM (**2**) as the major product. A minor amount of Et-PCPM (**3**) is also formed in reactions with both ThnK and TokK (Fig. S1, ESI†). When (*S*)-[6-^{2}H]PCPM (**21b**) was incubated with each enzyme (Fig. 4 blue traces), the major product was unlabeled Me-PCPM (**2**), which closely matched the product formed in control reactions with unlabeled PCPM (**1**, Fig. 4 black traces). The formation of unlabeled product indicates that the pro-*S* deuterium is abstracted by 5′-dA• in both enzymes. The production of 5′-dA[2]H was also observed in reactions with (*S*)-[6-^{2}H]PCPM (**21b**), confirming this result.

© 2022 The Author(s). Published by the Royal Society of Chemistry

RSC Chem. Biol., 2022, **3**, 1028–1034 | **1031**

Scheme 2 Elaboration of β-lactams **14a** and **14b** to the corresponding PCPMs **21a** and **21b**. *Reagents and conditions*: (a) H$_2$ (1 atm), Pd/C, EtOAc, rt, 3 h; (b) iBuCO$_2$Cl, NEt$_3$, THF, 0 °C, 30 min, then CH$_2$N$_2$, Et$_2$O, 0 °C to rt, 3.5 h; (c) *hν*, THF, H$_2$O, rt, 18 h; (d) CDI, CH$_3$CN, rt, 1 h, then Mg(mono-PNB malonate)$_2$, 60 °C, 18 h; (e) TBAF, AcOH, THF, 0 °C, 30 min; (f) MsN$_3$, DIPEA, CH$_3$CN, 0 °C to rt, 1 h; (g) Rh$_2$(OAc)$_4$, PhH, reflux, 30 min; (h) NaBH$_4$, MeOH/THF, −78 °C, 30 min; (i) MsCl, NEt$_3$, CH$_2$Cl$_2$, rt, 1 h; (j) pantetheine, NEt$_3$, CH$_3$CN, rt, 1 h, then HPLC separation; (k) H$_2$ (30 psi), Pd/C, THF, KHPO$_4$ (aq), pH 7, rt, 1 h.

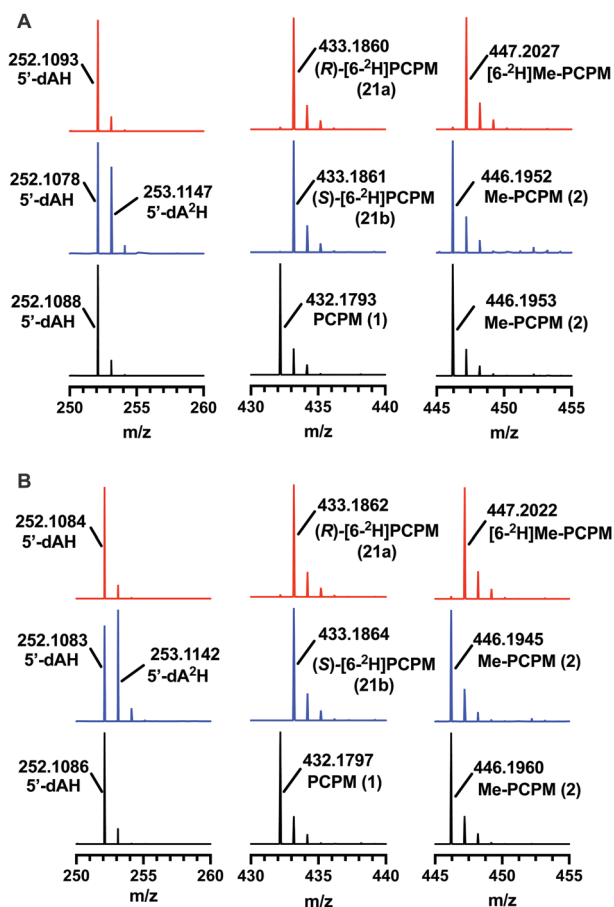**Fig. 4** Electrospray ionization (ESI) mass data from reactions with (A) TokK and (B) ThnK. Red traces are from reactions with (*R*)-[6-^{2}H]PCPM (**21a**), blue traces are from reactions with (*S*)-[6-^{2}H]PCPM (**21b**), black traces are from reactions with unlabeled PCPM (**1**). Calculated masses are as follows: 5′-dAH, 252.1091; 5′dA^{2}H, 253.1154; PCPM, 432.1799; [6-^{2}H$_1$]PCPM, 433.1862; Me-PCPM, 446.1955; [6-^{2}H$_1$]Me-PCPM, 447.2018.
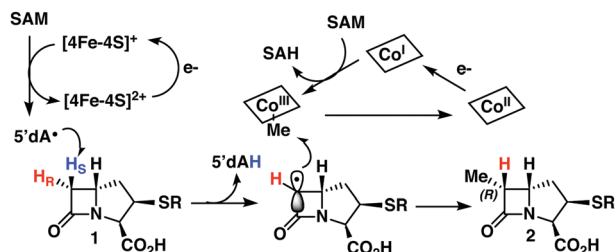
deuterium was retained in the product of the reaction. These reactions also produced unlabeled 5′-dAH in accord with pro-*S* hydrogen abstraction by 5′-dA•. The fact that reactions with TokK and ThnK gave virtually identical results reveals that the overall architecture of their active sites is highly conserved despite the differences in their kinetic profiles.[1] These results establish that both ThnK and TokK proceed with inversion of configuration at C6. The high specificity of both enzymes for the pro-*S* hydrogen indicates that the position of PCPM in the substrate-bound structure of TokK is not precisely poised for hydrogen abstraction. Rather, C6 of PCPM must move slightly in the active site to facilitate alignment of the pro-*S* hydrogen with 5′-dA•. This motion could also place the resulting C6 radical at a more ideal distance for methyl transfer from MeCbl. Although characterized examples are still quite limited, inversion of configuration seems to be more commonly the case for Cbl-dependent rSAM methylases, as this stereochemical process is shared by Fom3,[12–14] as well as GenD1,[42] and MoeK.[43] The latter two enzymes have been assigned a function using traditional knock-out experiments rather than through *in vitro* study, but as they both catalyze methylation of chiral centers, their stereochemical course can be directly inferred. In contrast, as mentioned above, GenK[44] has been shown to proceed with overall retention of configuration,[15] suggesting that the active site of a Cbl-dependent rSAM methylase can accommodate the cofactors in varying orientations. Interestingly, the specificity of GenK appears to be weakened when the preferred hydrogen is replaced with deuterium. In this reaction, approximately 20% of the accumulated product is deuterated, potentially due to a primary kinetic isotope effect in the initial H-abstraction step.[15] This phenomenon is observed to a lesser degree in both TokK and ThnK, which accumulate *ca.* 7% and 4% of [6-^{2}H]Me-PCPM, respectively, when (*S*)-[6-^{2}H]PCPM (**21b**) is used.

Conversely, when (*R*)-[6-^{2}H]PCPM (**21a**) was used (Fig. 4 red traces), the major product was [6-^{2}H]Me-PCPM, showing that

Conclusions

Here we present the synthesis of deuterated PCPMs of high isotopic and stereochemical purity from diastereomeric [3-^{2}H]-aspartates

1032 | *RSC Chem. Biol.*, 2022, **3**, 1028–1034

© 2022 The Author(s). Published by the Royal Society of Chemistry

Scheme 3 Proposed mechanism of Cbl-dependent rSAM methylation by TokK and ThnK.

and their subsequent enzymatic analysis with both TokK and ThnK. These experiments lead to the mechanism proposed in Scheme 3, wherein the reductive cleavage of SAM generates 5′-dA•, which stereospecifically abstracts the pro-*S* hydrogen at C6 of PCPM. The resulting planar PCPM radical is methylated from the opposite face by MeCbl to give (6*R*)-Me-PCPM (2), affording inversion of absolute configuration at C6. Single-electron reduction of Cob(ɪɪ)alamin and subsequent methylation by SAM regenerates MeCbl for the next round of methylation. Comparison of the structures of TokK solved with and without bound substrate shows that only a few residues shift upon substrate binding, while the positions of the metallocofactors remain unchanged. Moreover, a single active site must accommodate the growing alkyl chain constructed by TokK and ThnK. While our stereochemical experiments only provide insight into the first methylation by both enzymes, they complement the structural characterization of TokK to give a more complete understanding of the interactions between reacting groups. PCPMs are anchored by the binding of the C3-carboxylate to Arg280, but the stereospecificity of hydrogen abstraction points to allowable motion of PCPM in the active site, and could suggest that the PCPM crystallized in the TokK active site is not precisely poised for methyl transfer. Potential PCPM mobility could also help to explain how a single enzyme can catalyze multiple methylations both at C6 and the newly introduced carbon. The kinetic differences between TokK and ThnK and the catalysis of three *vs.* two methyl transfers have been partially attributed to three amino acid substitutions proximal to the active site.[5] Taken together with previous kinetic and structural characterization of TokK, our stereochemical exploration of ThnK and TokK expands the limited understanding of methylation by the large and growing subfamily of Cbl-dependent rSAM enzymes and provides further insight into the even smaller subset of sequential methylases.

Author contributions

All authors were involved in conceptualizing experiments, which were carried out by M. S. L. and E. K. S. All authors were involved in data analysis, as well as writing and editing the manuscript.

Conflicts of interest

There are no conflicts to declare.

Notes and references

1 E. K. Sinner, M. S. Lichstrahl, R. Li, D. R. Marous and C. A. Townsend, *Chem. Commun.*, 2019, **55**, 14934–14937.

2 D. R. Marous, E. P. Lloyd, A. R. Buller, K. A. Moshos, T. L. Grove, A. J. Blaszczyk, S. J. Booker and C. A. Townsend, *Proc. Natl. Acad. Sci. U. S. A.*, 2015, **112**, 10354.

3 J. M. Williamson, E. Inamine, K. E. Wilson, A. W. Douglas, J. M. Liesch and G. Albers-Schonberg, *J. Biol. Chem.*, 1985, **260**, 4637–4647.

4 J. Shoji, H. Hinoo, R. Sakazaki, N. Tsuji, K. Nagashima, K. Matsumoto, Y. Takahashi, S. Kozuki, T. Hattori, E. Kondo and K. Tanaka, *J. Antibiot.*, 1982, **35**, 15–23.

5 H. L. Knox, E. K. Sinner, C. A. Townsend, A. K. Boal and S. J. Booker, *Nature*, 2022, **602**, 343–348.

6 M. R. Bauerle, E. L. Schwalm and S. J. Booker, *J. Biol. Chem.*, 2015, **290**, 3995–4002.

7 E. K. Sinner, D. R. Marous and C. A. Townsend, *ACS Bio Med Chem Au*, 2022, **2**, 4–10.

8 S. C. Wang, *Nat. Prod. Rep.*, 2018, **35**, 707–720.

9 Y. Wang, B. Schnell, S. Baumann, R. Müller and T. P. Begley, *J. Am. Chem. Soc.*, 2017, **139**, 1742–1745.

10 D. R. Houck, K. Kobayashi, J. M. Williamson and H. G. Floss, *J. Am. Chem. Soc.*, 1986, **108**, 5365–5366.

11 S. Sato, F. Kudo, S.-Y. Kim, T. Kuzuyama and T. Eguchi, *Biochemistry*, 2017, **56**, 3519–3522.

12 M. I. McLaughlin and W. A. van der Donk, *Biochemistry*, 2018, **57**, 4967–4971.

13 S. Sato, F. Kudo, T. Kuzuyama, F. Hammerschmidt and T. Eguchi, *Biochemistry*, 2018, **57**, 4963–4966.

14 B. Wang, A. J. Blaszczyk, H. L. Knox, S. Zhou, E. J. Blaesi, C. Krebs, R. X. Wang and S. J. Booker, *Biochemistry*, 2018, **57**, 4972–4984.

15 H. J. Kim, Y. Liu, R. M. McCarty and H. Liu, *J. Am. Chem. Soc.*, 2017, **139**, 16084–16087.

16 J. Bridwell-Rabb, B. Li and C. L. Drennan, *ACS Bio Med Chem Au*, 2022, DOI: **acsbiomedchemau.1c00051**.

17 J. Bridwell-Rabb, A. Zhong, H. G. Sun, C. L. Drennan and H. Liu, *Nature*, 2017, **544**, 322–326.

18 H. L. Knox, P. Y.-T. Chen, A. J. Blaszczyk, A. Mukherjee, T. L. Grove, E. L. Schwalm, B. Wang, C. L. Drennan and S. J. Booker, *Nat. Chem. Biol.*, 2021, **17**, 485–491.

19 C. D. Fyfe, N. Bernardo-García, L. Fradale, S. Grimaldi, A. Guillot, C. Brewee, L. M. G. Chavas, P. Legrand, A. Benjdia and O. Berteau, *Nature*, 2022, **602**, 336–342.

20 A. Zhong, Y.-H. Lee, Y. Liu and H. Liu, *Biochemistry*, 2021, **60**, 537–546.

21 S. Pierre, A. Guillot, A. Benjdia, C. Sandström, P. Langella and O. Berteau, *Nat. Chem. Biol.*, 2012, **8**, 957–959.

© 2022 The Author(s). Published by the Royal Society of Chemistry

RSC Chem. Biol., 2022, **3**, 1028–1034 | **1033**

22 A. J. Blaszczyk, A. Silakov, B. Zhang, S. J. Maiocco, N. D. Lanz, W. L. Kelly, S. J. Elliott, C. Krebs and S. J. Booker, *J. Am. Chem. Soc.*, 2016, **138**, 3416–3426.

23 M. I. Radle, D. V. Miller, T. N. Laremore and S. J. Booker, *J. Biol. Chem.*, 2019, **294**, 11712–11725.

24 M. J. Bodner, R. M. Phelan and C. A. Townsend, *Org. Lett.*, 2009, **11**, 3606–3609.

25 A. Soicke, C. Reuter, M. Winter, J.-M. Neudörfl, N. Schlörer, R. Kühne and H.-G. Schmalz, *Eur. J. Org. Chem.*, 2014, 6467–6480.

26 R. Takeda, H. Abe, N. Shibata, H. Moriwaki, K. Izawa and V. A. Soloshonok, *Org. Biomol. Chem.*, 2017, **15**, 6978–6983.

27 P. Ji, Y. Zhang, Y. Dong, H. Huang, Y. Wei and W. Wang, *Org. Lett.*, 2020, **22**, 1557–1562.

28 S. W. Chun and A. R. H. Narayan, *ACS Catal.*, 2020, **10**, 7413–7418.

29 K. M. Lee, K. Ramalingam, J. K. Son and R. W. Woodard, *J. Org. Chem.*, 1989, **54**, 3195–3198.

30 K. Kusuda, J. Inanaga and M. Yamaguchi, *Tetrahedron Lett.*, 1989, **30**, 2945–2948.

31 Y. Gao and C. M. Zepp, *Tetrahedron Lett.*, 1991, **32**, 3155–3158.

32 R. Hili, V. Rai and A. K. Yudin, *J. Am. Chem. Soc.*, 2010, **132**, 2889–2891.

33 F. A. Davis, C. H. Liang and H. Liu, *J. Org. Chem.*, 1997, **62**, 3796–3797.

34 Y. Gao and K. B. Sharpless, *J. Am. Chem. Soc.*, 1988, **110**, 7538–7539.

35 K. B. Sharpless and Y. Gao, *US Pat.*, US5321143A, 1994.

36 R. W. Feenstra, E. H. M. Stokkingreef, R. J. F. Nivard and H. C. J. Ottenheijm, *Tetrahedron*, 1988, **44**, 5583–5595.

37 R. V. Hoffman and K. Hwa-Ok, *Tetrahedron Lett.*, 1990, **31**, 2953–2956.

38 L. Decuyper, J. Franceus, S. Dhaene, M. Debruyne, K. Vandoorne, N. Piens, G. Dewitte, T. Desmet and M. D'hooghe, *ACS Omega*, 2018, **3**, 15235–15245.

39 J. Fetter, K. Lempert, T. Gizur, J. Nyitrai, M. Kajtár-Peredy, G. Simig, G. Hornyák and G. Doleschall, *J. Chem. Soc., Perkin Trans. 1*, 1986, 221–227.

40 D. W. Brooks, L. D.-L. Lu and S. Masamune, *Angew. Chem., Int. Ed. Engl.*, 1979, **18**, 72–74.

41 E. K. Sinner and C. A. Townsend, *Methods Enzymol.*, 2021, **669**, 29–44.

42 C. Huang, F. Huang, E. Moison, J. Guo, X. Jian, X. Duan, Z. Deng, P. F. Leadlay and Y. Sun, *Chem. Biol.*, 2015, **22**, 251–261.

43 B. Ostash, E. H. Doud, C. Lin, I. Ostash, D. L. Perlstein, S. Fuse, M. Wolpert, D. Kahne and S. Walker, *Biochemistry*, 2009, **48**, 8830–8841.

44 H. J. Kim, R. M. McCarty, Y. Ogasawara, Y. N. Liu, S. O. Mansoorabadi, J. LeVieux and H. W. Liu, *J. Am. Chem. Soc.*, 2013, **135**, 8093–8096.